

High-resolution observations of SN 2001gd in NGC 5033

M.A. Pérez-Torres^{1*}, A. Alberdi¹, J.M. Marcaide², M.A. Guerrero¹, P. Lundqvist³, I.I. Shapiro⁴, E. Ros⁵, L. Lara^{6,1}, J.C. Guirado², K.W. Weiler⁷, C.J. Stockdale⁷

¹*Instituto de Astrofísica de Andalucía, CSIC, Apdo. Correos 3004, E-18080 Granada, Spain*

²*Departamento de Astronomía y Astrofísica, Universidad de Valencia, E-46100 Burjassot, Spain*

³*Stockholm Observatory, AlbaNova, Roslagstullsbacken 21, SE-10691 Stockholm, Sweden*

⁴*Harvard-Smithsonian Center for Astrophysics, 60 Garden St. MS 51, Cambridge, MA 02138, USA*

⁵*Max-Planck-Institut für Radioastronomie, Auf dem Hügel 69, D-53121 Bonn, Germany*

⁶*Departamento de Física Teórica y del Cosmos, Universidad de Granada, E-18071 Granada, Spain*

⁷*Naval Research Laboratory, Code 7213, Washington, DC 20375-5320, USA*

Accepted 2005 April 11. Received 2005 April 7; in original form 2004 November 10

ABSTRACT

We report on 8.4 GHz VLBI observations of SN 2001gd in the spiral galaxy NGC 5033 made on 26 June 2002 (2002.48) and 8 April 2003 (2003.27). We used the interferometric visibility data to estimate angular diameter sizes for the supernova by model fitting. Our data nominally suggests a relatively strong deceleration for the expansion of SN 2001gd, but we cannot dismiss the possibility of a free supernova expansion. From our VLBI observations on 8 April 2003, we inferred a minimum total energy in relativistic particles and magnetic fields in the supernova shell of $E_{\min} = (0.3-14) \times 10^{47}$ ergs, and a corresponding equipartition average magnetic field of $B_{\min} = (50-350)$ mG. We also present multiwavelength VLA measurements of SN 2001gd made at our second VLBI epoch at the frequencies of 1.4, 4.9, 8.4, 15.0, 22.5, and 43.3 GHz. The VLA data are well fit by an optically thin, synchrotron spectrum ($\alpha = -1.0 \pm 0.1$; $S_{\nu} \propto \nu^{\alpha}$), partially absorbed by thermal plasma. We obtain a supernova flux density of (1.02 ± 0.05) mJy at the observing frequency of 8.4 GHz for the second epoch, which results in an isotropic radio luminosity of $(6.0 \pm 0.3) \times 10^{36}$ ergs s⁻¹ between 1.4 and 43.3 GHz, at an adopted distance of 13.1 Mpc. Finally, we report on an *XMM-Newton* X-ray detection of SN 2001gd on 18 December 2002. The supernova X-ray spectrum is consistent with optically thin emission from a soft component (associated with emission from the reverse shock) at a temperature around 1 keV. The observed flux corresponds to an isotropic X-ray luminosity of $L_X = (1.4 \pm 0.4) \times 10^{39}$ ergs s⁻¹ in the 0.3–5 keV band. We suggest that both radio and X-ray observations of SN 2001gd indicate that a circumstellar interaction similar to that displayed by SN 1993J in M 81 is taking place.

Key words: galaxies: individual: NGC 5033 – radio continuum: stars – supernovae: individual: SN 2001gd – X-rays: individual SN 2001gd

1 INTRODUCTION

SN 2001gd in NGC 5033 was discovered by Nakano et al. (2001) on 24.82 November 2001; its explosion date is uncertain. The supernova had a visual magnitude then of 14.5, and was located $\sim 3'$ north-northwest of the nucleus of NGC 5033. Nakano et al. (2001) reported the following position for SN 2001gd: $\alpha=13h13m23s.89$, $\delta=+36^{\circ}38'17''$.7 (equinox J2000.0). They also reported that there was no star visible at the above position on earlier frames taken be-

tween 1996 and April 2001. An optical spectrum obtained by P. Berlind on 4.52 December 2001 (Matheson et al. 2001), showed SN 2001gd to be a Type IIb supernova well past maximum light. Matheson et al. (2001) pointed out that the spectrum was almost identical to that of SN 1993J obtained on day 93 after explosion (Matheson et al. 2000). Since SN 1993J was a strong radio emitter, it was natural to expect SN 2001gd would also be a strong radio emitter. Stockdale et al. (2002) detected SN 2001gd on 8 February 2002 at cm-wavelengths with the Very Large Array (VLA). Their continual monitoring of SN 2001gd since its first radio detection has confirmed that SN 2001gd is similar in its ra-

* E-mail: torres@iaa.es

dio properties to SN 1993J (peak luminosity at 6 cm, time to 6 cm peak, spectral index; Stockdale et al. 2003), as in its optical properties. Given the similarities between the optical spectrum of SN 2001gd on 4.52 December 2001 and that of SN 1993J at an age of 93 days (Matheson et al. 2001), we assume throughout our paper that the supernova exploded 93 days before 5 December, therefore fixing that event at $t_0 = 3$ September 2001.

A preliminary report on our radio findings is presented in Pérez-Torres et al. (2005). Here, we present the results of our two-epoch VLBI observing campaign on SN 2001gd, complemented with VLA observations and *XMM-Newton* archival X-ray data. The paper is organized as follows: we report on our VLBI and VLA radio observations, and on *XMM-Newton* archival X-ray data in Sect. 2; we present our VLBI images of SN 2001gd in Sect. 3; we present and discuss our results in Sect. 4. We summarize our main conclusions in Sect. 5. We assume throughout our paper a distance of 13.1 Mpc to the host galaxy of SN 2001gd, NGC 5033, based on its redshift ($z = 0.002839$; Falco et al. 1999) and assumed values of $H_0 = 65 \text{ km s}^{-1} \text{ Mpc}^{-1}$ and $q_0 = 0$. At this distance, 1 mas corresponds to a linear size of 0.063 pc.

2 OBSERVATIONS AND DATA REDUCTION

2.1 VLBI measurements

We observed SN 2001gd on 26 June 2002 (2002.48) at a frequency of 8.4 GHz, using a VLBI array that included the following 12 antennas (diameter, location): The VLBA (25 m, 10 identical antennas across the USA), Green Bank (100 m, WV, USA), and Effelsberg (100 m, Germany). We also observed SN 2001gd on 8 April 2003 (2003.27) at the same frequency with the above array, complemented with the phased-VLA (130 m-equivalent, NM, USA), and Medicina and Noto (32 m each, Italy). However, for our second epoch we had to discard three antennas (Hancock, North Liberty, and Noto) due to the poor quality of their data. The duration of each observing run was eight hours. The telescope systems recorded right-hand circular polarization (RCP), and used a bandwidth of 64 MHz, except for the VLA (bandwidth of 50 MHz). The data were correlated at the VLBA Correlator of the National Radio Astronomy Observatory (NRAO) in Socorro (NM, USA). The correlator used an averaging time of 2 s.

Since previous VLA observations of SN 2001gd showed it to be fainter than 6 mJy at 8.4 GHz, our VLBI observations were carried out in phase-reference mode. SN 2001gd and the nearby International Celestial Reference Frame (ICRF) source J1317+34 ($z = 1.050$; Hewitt & Burbidge 1989) were alternately observed through each eight-hour long VLBI run. The observations consisted of ~ 145 s scans on SN 2001gd and ~ 95 s scans on J1317+34, plus ~ 60 additional seconds of antenna slew time to make a duty cycle of ~ 300 s. In each observing run, the total on-source time was ≈ 4.2 h and ≈ 2.5 h for SN 2001gd and J1317+34, respectively. J1317+34 was also used as the amplitude calibrator for SN 2001gd. The sources 4C 39.25 and J1310+32 (both ICRF sources) were observed as fringe finders.

The correlated data were analyzed using the Astronomical Image Processing System (*AIPS*). The visibility amplitudes were calibrated using the system temperature and gain

information provided for each telescope. The instrumental phase and delay offsets among the 8 MHz baseband converters in each antenna were corrected using a phase calibration determined from observations of 4C 39.25 and J1310+32, for our VLBI observations on 26 June 2002 and 8 April 2003, respectively. We fringe-fit the data for the calibrator J1317+34 in a standard manner; these data were then exported to the Caltech program DIFMAP (Shepherd et al. 1995) for imaging purposes. The final source image obtained for J1317+34 was then included as an input image in a new round of fringe-fitting for J1317+34 within *AIPS*. In this way, the results obtained for the phase delays and delay-rates for J1317+34 were nearly structure-free. These new values were then interpolated and applied to the source SN 2001gd using *AIPS* standard procedures. The SN 2001gd data were then transferred into the DIFMAP program. We used standard phase self-calibration techniques using a time interval of 3 minutes, to obtain the images shown in Sect. 3.

2.2 VLA measurements

Our second observing epoch (2003.27) included the phased-VLA (in D-configuration) as an element of our VLBI array. We allocated about one hour of the VLA time to determine the radio spectrum of SN 2001gd. We observed at 1.4, 4.9, 8.4, 15.0, 22.5, and 43.3 GHz, in standard continuum mode. We observed in both senses of circular polarization and each frequency band was split into two intermediate frequencies (IFs), of 50 MHz bandwidth each. We used 3C 286 as the primary flux calibrator (assumed of constant flux density) at all frequencies. We observed SN 2001gd phase-referenced to J1310+32 (a nearby VLA phase-calibrator source) at all bands, except at 8.4 GHz, for which we used our VLBI amplitude calibrator, J1317+34, as the phase-reference source. J1310+32 and J1317+34 served also as the phase-reference sources for the system calibration. The flux densities reported here were obtained by combining the data from both IFs at each frequency band. As with our VLBI data, we used standard calibration and hybrid mapping techniques to obtain a VLA image of SN 2001gd and its host galaxy, NGC 5033, at the observing frequency of 8.4 GHz (see Fig. 1).

2.3 Two-epoch *XMM-Newton* X-ray observations

NGC 5033 was observed with the *XMM-Newton Observatory* on 2 July 2001 (PI: Turner, Obs. ID: 0112551301) and on 18 December 2002 (PI: Quataert, Obs. ID: 0094360501). Both observations used the EPIC/MOS1, EPIC/MOS2, and EPIC/pn CCD cameras (Strüder et al. 2001; Turner et al. 2001); the two EPIC/MOS cameras were operated in the Prime Full-Window Mode, while the EPIC/pn camera was operated in the Extended Prime Full-Window Mode. The useful exposure times were ~ 7.6 ks and ~ 11.6 ks for the EPIC/MOS cameras and ~ 4.0 ks and ~ 10.0 ks for the EPIC/pn camera for the observations ID 0112551301 and 0094360501, respectively. The observation ID 0112551301 used the Thin Filter for the EPIC/MOS observations; the Medium Filter was used for all the other observations.

We retrieved the *XMM-Newton* pipeline products from

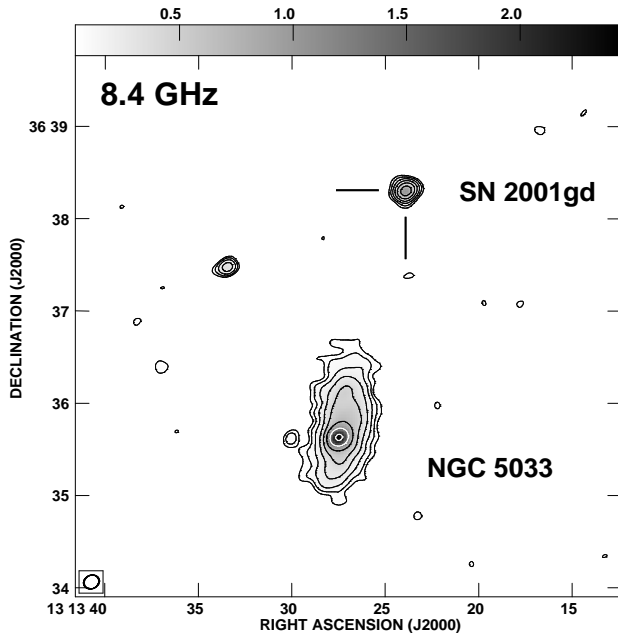


Figure 1. Hybrid image of the galaxy NGC 5033 and its supernova SN 2001gd made at 8.4 GHz with the Very Large Array (VLA), from observations on 8 April 2003. The contours are $(3, 3\sqrt{3}, 9, \dots) \times 16 \mu\text{Jy beam}^{-1}$, the off-source rms flux density per beam. The peak of brightness of the image corresponds to the nucleus of NGC 5033 and is $2.44 \text{ mJy beam}^{-1}$. The supernova is the bright point-like source northwards of the nucleus of NGC 5033. The principal dimensions (full width at half maximum) of the restoring beam are $10\text{''}1 \times 8\text{''}7$, with the beam's major axis oriented along a position angle of -61° (see inset in the lower left hand corner). $1''$ in the image corresponds to a linear size of 64 pc.

the *XMM-Newton* Science Archive¹. Initial processing and analysis were performed using the *XMM-Newton* Science Analysis Software (SAS ver. 6.0.0) and the calibration files from the Calibration Access Layer available on 13 April 2004. Subsequent spectral analysis was carried out with XSPEC.

We examined the light curve of the EPIC/MOS and EPIC/pn in the energy range above 10 keV to assess the effect of any high energy particle flux on the background level. Although the light curve of the observation ID 0094360501 on 18 December 2002 does not show any period of enhanced background, the observation ID 0112551301 on 2 July 2001 is severely affected, with a background level 40 times higher than on the 18 December 2002 observation. Finally, the data were filtered to remove poor event grades (most likely spurious X-ray events).

We extracted images from the EPIC/MOS and EPIC/pn observations in different energy bands with pixel size of $1''$. The images extracted from the observation on 2 July 2001 do not show any X-ray source at the location of SN 2001gd. On the other hand, the image in the 0.25–2.5 keV band extracted from the observation on 18 December 2002 (Fig. 2) does show a compact, soft X-ray source at

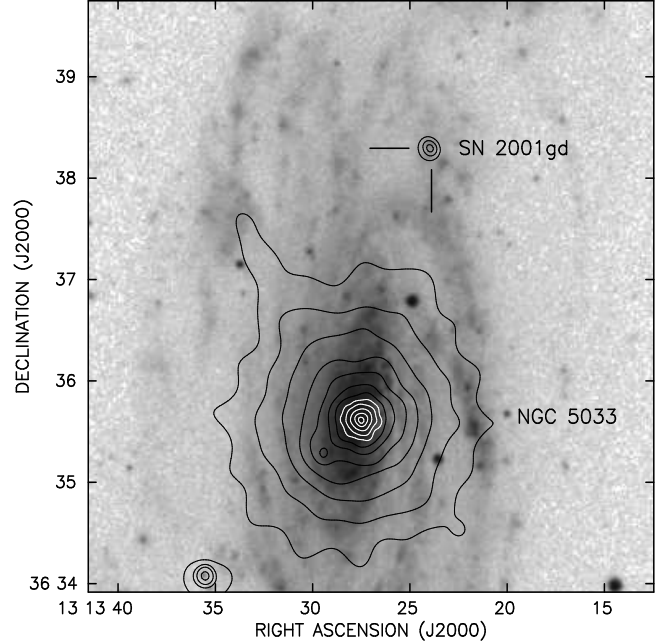


Figure 2. Contours of soft 0.25–2.5 keV X-rays from SN 2001gd overlaid on a Second-Epoch Digitized Sky Survey (DSS-2) Blue plate of NGC 5033. The X-ray image was extracted from the 18 December 2002 *XMM-Newton* observation of NGC 5033 (Obs. ID 0094360501). The EPIC/MOS and EPIC/pn images have been combined to obtain a higher S/N image. The raw EPIC image has been further adaptively smoothed using Gaussian profiles with FWHM ranging from $1\text{''}5$ to $9''$. The three contours in the image for SN 2001gd are drawn at $(3, 8, \text{ and } 13) \times 0.15 \text{ cnts/arcsec}^2$, the image off-source rms.

the location of SN 2001gd, with 19 ± 5 counts in the 0.3–2.0 keV band. In the energy band above 2 keV, there are only 2 ± 2 counts, which corresponds to a hardness ratio of $0.1^{+0.2}_{-0.1}$ between the energy band above 2 keV and the total *XMM-Newton* energy band. The facts that the pre-supernova observation yielded a non-detection and the post-supernova observation yielded a detection, coupled with the spatial coincidence and soft X-ray spectrum imply that the X-ray source is SN 2001gd, and that the supernova explosion likely happened after 2 July 2001.

3 VLBI IMAGES OF SN 2001GD

We used phase-reference techniques at both VLBI epochs to obtain images of SN 2001gd. The use of phase-referencing allows detection and imaging of very faint sources like supernovae, as it effectively increases the coherence time from minutes to hours (e.g., Beasley & Conway 1995). In our case, we made phase-reference observations of our target source, SN 2001gd, with respect to the relatively strong, nearby QSO J1317+34, which is $2^{\circ}22'$ distant.

We display in Fig. 3 our 8.4 GHz VLBI image of J1317+34 on 26 June 2002. The source shows a one-sided core-jet structure at milliarcsecond (mas) scales, with the jet extending northwards to ~ 9 mas. As mentioned in Sect. 2.1, we subtracted at each epoch the phase contribution of J1317+34 (due to its extended structure) from

¹ The *XMM-Newton* Science Archive is supported by ESA and can be accessed at <http://xmm.vilspa.esa.es>

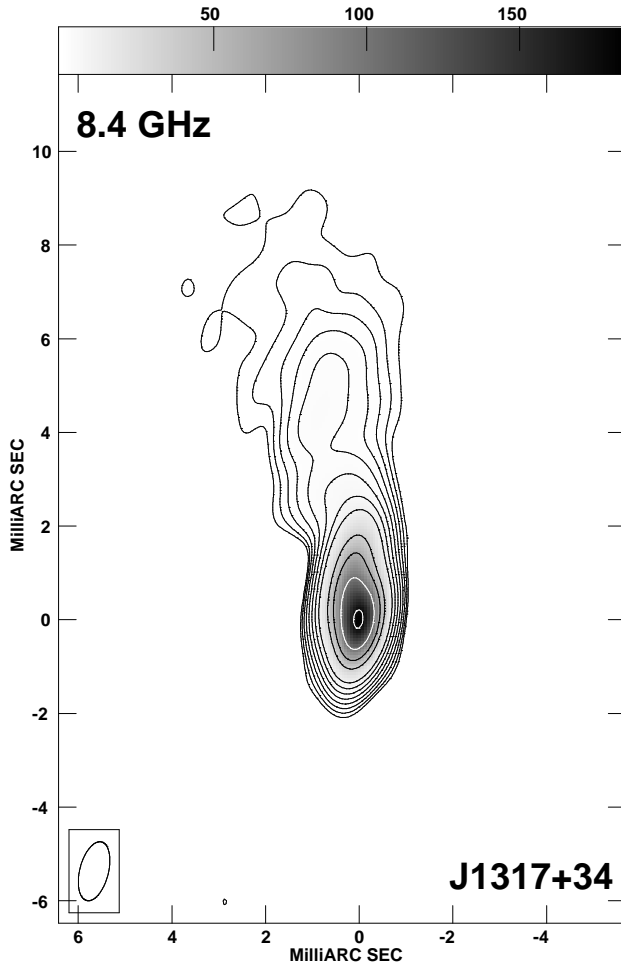


Figure 3. 8.4 GHz Very-Long-Baseline Interferometry (VLBI) image of J1317+34 on 26 June 2002. The contours are $(3.3\sqrt{3}, 9, \dots) \times 80 \mu\text{Jy beam}^{-1}$, the off-source rms flux density per beam. The peak of brightness of the image is $184 \text{ mJy beam}^{-1}$ and the restoring beam (bottom left in the image) is $1.29 \text{ mas} \times 0.61 \text{ mas}$ at a position angle of $-14^\circ 3$. The total flux density recovered in the image is $\sim 0.33 \text{ Jy}$. North is up and east is left. One milliarcsecond in the image corresponds to a linear size of 8.5 pc .

the fringe phase, and used the position of its phase-center (essentially coincident with the peak of the brightness distribution), as our reference point for phase-reference imaging.

Figure 4 shows our VLBI images of SN 2001gd, which showed no structure at both epochs. The coordinates of the supernova are offset from those provided by the VLA (Stockdale et al. 2002), and used as *a priori* VLBI coordinates in the correlator, for the supernova position, by a mere ~ 3 mas in right ascension and ~ 1 mas in declination. Since the standard error of the VLA position provided by Stockdale et al. (2002) was 0.2 arcsec in each coordinate, the (small) differences between the VLBI and VLA determined coordinates would be a highly improbable event. It is more likely that the VLA uncertainties quoted by Stockdale et al. (2002) were far too conservative. Indeed, a reanalysis of the 8.4 GHz VLA observations of Stockdale et al. (2002) results

in 1σ uncertainties of $0.015\text{--}0.0020$ arcsec (C. Stockdale, private communication) for the VLA position of SN 2001gd, about a factor of ten smaller than the uncertainties quoted in Stockdale et al. (2002).

4 RESULTS AND DISCUSSION

4.1 Radio light curve and spectral behaviour

Simultaneous multiwavelength radio observations of supernovae are important to help characterize the relevant physical processes taking place. Since we were granted VLA observing time for our second VLBI epoch on 8 April 2003 we were able to characterize the radio spectral energy distribution of SN 2001gd. The flux density measurement error given for the VLA measurements in Table 1 represents one statistical standard deviation, and is a combination of the off-source rms in the image and a fractional error, ϵ , included to account for the normal inaccuracy of VLA flux density calibration and possible deviations of the primary calibrator from an absolute flux density scale: the final errors, σ_f , as listed in Table 1, are taken as $\sigma_f^2 = (\epsilon S_0)^2 + \sigma_0^2$ (see, e.g., Stockdale et al. 2003), where S_0 is the measured flux density, σ_0 is the off-source rms at a given frequency, and $\epsilon=0.10$ at 1.4 GHz, 0.05 at 4.9 GHz, 0.05 at 8.4 GHz, 0.075 at 15.0 GHz, and 0.10 at 22.5 and 43.3 GHz. We fit our data using an implementation of the nonlinear weighted-least-squares Marquardt-Levenberg algorithm. We plot in Fig. 5 two model fits to the data in Table 1. The solid line corresponds to a fit to the data with a power-law spectrum that is partially suppressed by free-free absorption from a homogeneous screen of ionised gas [$S_\nu = S_1 \nu^\alpha \exp(-\tau_{\text{ff},\nu})$], where S_1 is the flux density at 1 GHz, in mJy; ν is the observing frequency, in GHz; and $\tau_{\text{ff},\nu} = A \nu^{-2.1}$ is the free-free optical depth at the observing frequency ν . The dashed-dotted line corresponds to a pure synchrotron spectrum fit. For our first model, we obtain the following weighted-least-squares (“best-fit”) values for the parameters: $S_1 = (9.1 \pm 1.6) \text{ mJy}$, $\alpha = -1.0 \pm 0.1$, $A = (1.0 \pm 0.3) \text{ GHz}^{-2.1}$. (The quoted uncertainties correspond to 1σ .) The observed spectral index is typical of the optically thin phase of Type II supernovae. The corresponding optical depth at 8.4 GHz is $\tau_{\text{ff},8.4} = (1.1 \pm 0.3) \times 10^{-2}$. This estimate can be used to constrain the electron temperature, $T_e = 10^5 T_5 \text{ K}$, and mass-loss rate parameter of the supernova progenitor, \dot{M}/v_w . (Each letter symbol with a subscript indicates the value of the corresponding quantity in units of 10 to the power given by the subscript; for example, T_5 above denotes T_e in units of 10^5 K.) Indeed, for a steady presupernova mass loss rate, $\dot{M} = 10^{-5} \dot{M}_{-5} \text{ M}_\odot \text{ yr}^{-1}$, and wind speed, $v_w = 10 v_{10} \text{ km s}^{-1}$, the free-free absorption optical depth of the unshocked ionised gas is (Lundqvist & Fransson 1988)

$$\tau_{\text{ff},\nu} \approx 0.17 g_{\text{ff}} \mu T_5^{-3/2} \nu^{-2} \dot{M}_{-5}^2 v_{10}^{-2} r_{16}^{-3} \quad (1)$$

where ν is the frequency in GHz, $r = 10^{16} r_{16} \text{ cm}$, is the radius of the circumstellar shock, g_{ff} is the free-free Gaunt factor, and $\mu = [1 + 2n(\text{He})/n(\text{H})]/[1 + 4n(\text{He})/n(\text{H})]$ is the mean molecular weight for the presupernova wind. For solar abundances, $n(\text{He})/n(\text{H}) = 0.1$ and $\mu = 0.86$, while for $n(\text{He})/n(\text{H}) = 1$, as may have been the case for SN 1993J

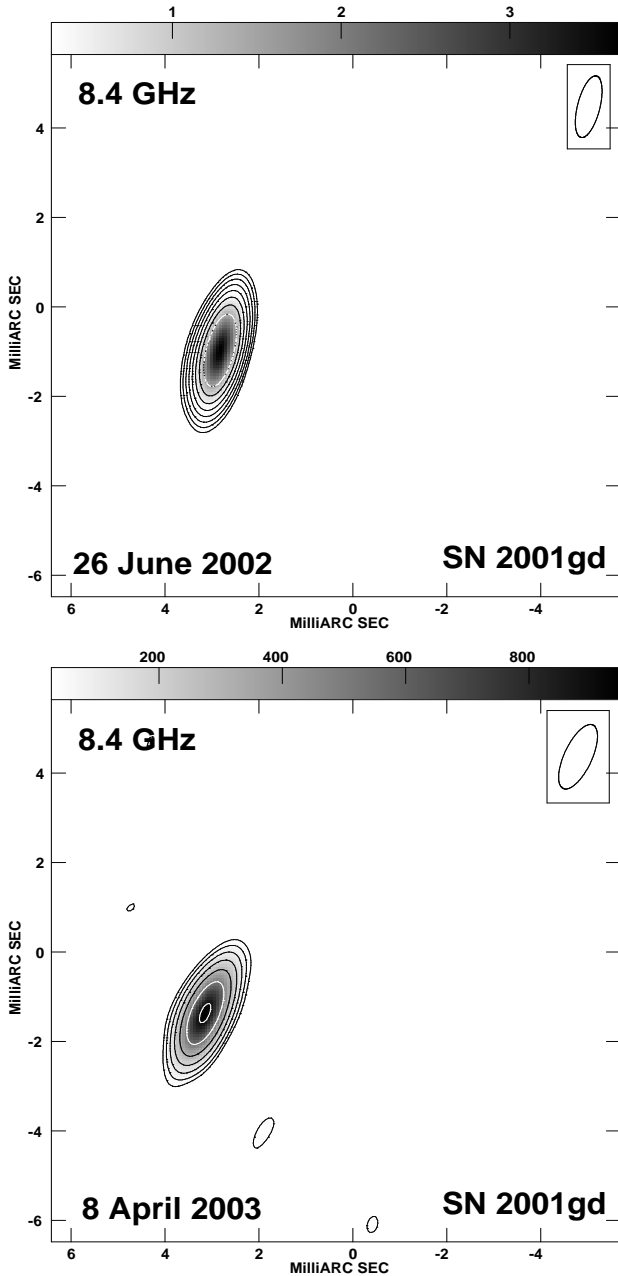


Figure 4. *Top:* Very-Long-Baseline Interferometry (VLBI) image of SN 2001gd on 26 June 2002. Contours are drawn at $(3, 3\sqrt{3}, 9, \dots) \times 10 \mu\text{Jy beam}^{-1}$, the off-source rms. The restoring beam (top right) is $1.41 \times 0.48 \text{ mas}^2$ at a position angle of $-13^\circ.4$. The peak of brightness is $3.64 \text{ mJy beam}^{-1}$, and the total flux density recovered for the supernova is 3.83 mJy . *Bottom:* Very-Long-Baseline Interferometry (VLBI) image of SN 2001gd on 8 April 2003. Contours are drawn at $(3, 3\sqrt{3}, 9, \dots) \times 11 \mu\text{Jy beam}^{-1}$, the off-source rms. The restoring beam (top right) is $1.55 \times 0.59 \text{ mas}^2$ at a position angle of $-23^\circ.7$. The peak of brightness is $944 \mu\text{Jy beam}^{-1}$, and the flux density recovered for the supernova is 1.02 mJy . In both panels, north is up and east is left; the origins are taken from the VLA observations.

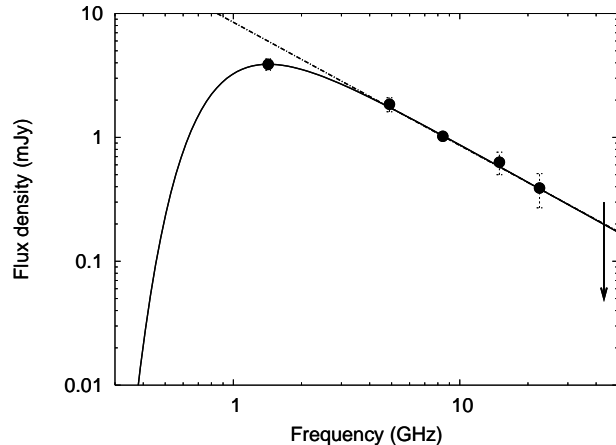


Figure 5. Model fits to the radio spectrum of SN 2001gd on 8 April 2003. The solid line corresponds to a synchrotron spectrum fit, partially suppressed by free-free absorption, whilst the dashed-dotted line corresponds to a pure synchrotron spectrum fit for all frequencies, except 1.4 GHz. The error bars denote $\pm 1\sigma$ values.

(Baron et al. 1994), $\mu=0.6$. Using $r_{16} = 3.6$ (see Sect. 4.3 below) and evaluating g_{ff} at 8.4 GHz, we obtain $\tau_{\text{ff},\nu} \approx 2.1 \times 10^{-4} (\mu/0.6) T_5^{-3/2} \dot{M}_{-5}^2 v_{10}^{-2}$. Fransson et al. (1996) and Fransson & Björnsson (1998) showed that $T_5 \approx 2$ and $(\dot{M}_{-5}/v_{10}) \approx 5$ were needed to explain the X-ray and radio emission of SN 1993J. Using the above values of T_5 and (\dot{M}_{-5}/v_{10}) for SN 2001gd on 8 April 2003, we obtain from Equation (1) $\tau_{\text{ff},8.4} \approx 2 \times 10^{-3}$, which is a factor of three too low to fit the lower end of our value for $\tau_{\text{ff},8.4}$. We explored the space of possibilities within 2σ of our best-fit values for the parameters S_1, α , and A (see above). We found very good matches for $\tau_{\text{ff},8.4}$ for the pairs of values $(T_e=3 \times 10^4 \text{ K}; \dot{M}=2.5 \times 10^{-5} \text{ M}_\odot \text{ yr}^{-1})$ and $(T_e=2 \times 10^5 \text{ K}; \dot{M}=1 \times 10^{-4} \text{ M}_\odot \text{ yr}^{-1})$. Unfortunately, the coupling of T_e and (\dot{M}/v_w) prevents us from favouring one pair of values over any other solely based on the radio observations, so we limit ourselves to pointing out that the values of T_e and \dot{M} for SN 2001gd are likely to be in the range $T_e=(3-20) \times 10^4 \text{ K}$, $\dot{M}=(2-10) \times 10^{-5} \text{ M}_\odot \text{ yr}^{-1}$. As we will see in Sect. 4.2, the available X-ray data favour models with $\dot{M} \lesssim 5 \times 10^{-5} \text{ M}_\odot \text{ yr}^{-1}$, which would imply electron temperatures of $T_e \lesssim 7 \times 10^4 \text{ K}$ to satisfy our radio observations.

4.2 X-ray emission from SN 2001gd

Models for the circumstellar interaction around supernovae (e.g., Fransson et al. 1996) predict the existence of two components in X-rays: a soft component associated with the reverse shock of the supernova, T_{rs} , and a hard component associated with the circumstellar shock, T_{cs} , e.g., SN 1995N (Mucciarelli et al. 2004). The 18 December 2002 ($t-t_0=472$ d) *XMM-Newton* observations of NGC 5033 can be used to investigate the circumstellar interaction around SN 2001gd and to estimate its X-ray luminosity. However, the spectrum has too small a number of counts to allow spectral fitting. Instead, we compared the count rate and hardness ratio of the observed *XMM-Newton* EPIC/pn spec-

Table 1. Results from VLA observations on 8 April 2003

Source Name	Flux density (mJy)					
	43.3 GHz	22.5 GHz	15.0 GHz	8.4 GHz	4.9 GHz	1.4 GHz
SN 2001gd	$\lesssim 0.30^{\dagger}$	0.39 ± 0.12	0.63 ± 0.13	1.02 ± 0.05	1.85 ± 0.24	3.89 ± 0.40
1310 + 323 ⁽¹⁾	2584 ± 258	2911 ± 291	2397 ± 178	—	1656 ± 83	1535 ± 154
J1317 + 34 ⁽²⁾	—	—	—	384 ± 19	—	—

⁽¹⁾ Phase and secondary flux density calibrator at all frequencies, except at 8.4 GHz. ⁽²⁾ Phase and secondary flux density calibrator at 8.4 GHz. [†] The quoted flux density at 43.3 GHz is an upper limit, corresponding to three times the off-source rms noise in the image. The quoted uncertainty for each flux density value corresponds to 1σ (see Sect. 4.1 for details).

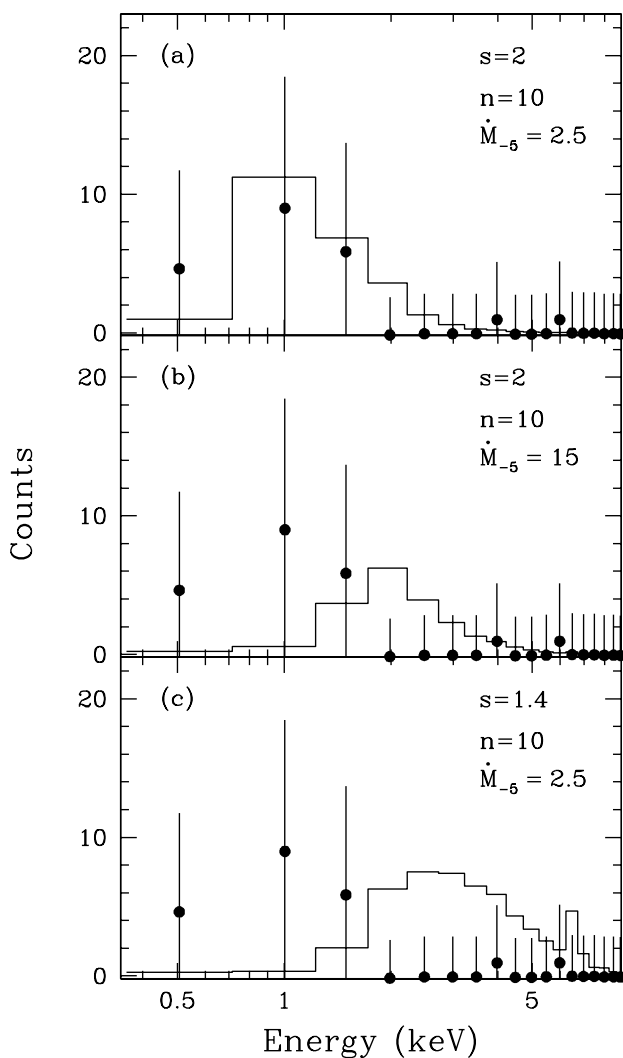


Figure 6. *XMM-Newton* EPIC/pn spectrum of SN 2001gd on 18 December 2002, overplotted by thin plasma X-ray emission models for a supernova radiative reverse shock (Fransson et al. 1996). The different sets of parameters are displayed in the corresponding panel. The uncertainties shown are one statistical standard deviation. The energy bin-width is 0.5 keV; therefore, 1 cnt in the spectrum corresponds to $\sim 2.0 \times 10^{-4}$ cnt s $^{-1}$ keV $^{-1}$.

trum with these implied from the analytical models for X-ray supernovae by Fransson et al. (1996). Figure 6 shows the *XMM-Newton* spectrum of SN 2001gd on 18 December 2002, overplotted by several optically thin plasma X-ray emission models. According to these models, both column density absorption and electron temperature are sensitive to the circumstellar density profile ($\rho_{\text{csm}} \sim r^{-s}$), ejecta density profile ($\rho_{\text{ej}} \sim r^{-n}$), shock speed ($v_{\text{sh}} = 10^4 v_4$ km s $^{-1}$), and mass-loss rate ($\dot{M} = 10^{-5} \dot{M}_{-5} M_{\odot}$ yr $^{-1}$). As for the expansion velocity, H $_{\alpha}$ spectra taken on December 2001 and January 2002, indicate $v_{\text{HWHM}} \approx 7800 \pm 1000$ km s $^{-1}$ (T. Matheson, private communication). Considering a likely supernova deceleration from this date to the time when the X-ray observations were obtained, we adopted a supernova shock speed of $v_4 = 0.6$ on 18 December 2002. We also kept fixed the presupernova wind speed at $v_{10} = 1$, while we varied s , n , and \dot{M} to investigate their effects on the X-ray emission. We note that the analytical models of Fransson et al. (1996) do not predict the exact amount of X-ray luminosity, but the reverse shock total luminosity, L_{rs} . A close inspection of their results indicates that the X-ray luminosity is $\sim 20\%$ of L_{rs} , and thus we adopted an X-ray luminosity of this fraction of L_{rs} to estimate the *XMM-Newton* EPIC/pn count rate.

The supernova model that shows hardness ratio and X-ray luminosity most consistent with the *XMM-Newton* spectrum of SN 2001gd on 18 December 2002 has $kT_{\text{rs}} \approx 1.1$ keV, $s=2$, $n=10$, and $\dot{M}_{-5}=2.5$. For illustration purposes, we compare in Fig. 6 the spectral shape of this model (top panel) with the observed X-ray spectrum. The above parameters agree well with what is expected for a supernova radiative reverse shock (Fransson et al. 1996). Our value of $\dot{M}_{-5}=2.5$ for the mass-loss rate of SN 2001gd from the X-ray observations may be compared with the value of $\dot{M}_{-5}=3$ obtained by Stockdale et al. (2003) from their radio light curve modelling, and with our own estimates in Sect. 4.1. The corresponding column density of the cooling shell between the reverse shock and the contact surface is $N_{\text{cool}} = 5.5 \times 10^{21}$ cm $^{-2}$, and that of the circumstellar shock is $N_{\text{cs}} = 1.6 \times 10^{21}$ cm $^{-2}$. We note that the supernova shock speed, v_{sh} , and the ejecta density profile, n , are coupled, so that different combinations within a certain range of these parameters reproduce the observed hardness ratio and count rate. Models with supernova shock speeds as high as $v_4 \approx 1.2$, would require $n \approx 14$ to reproduce the observed hardness ratio, but result in unreasonably high *XMM-Newton* EPIC/pn count rates. On the other hand, models with supernova shock speeds as low as $v_4 \approx 0.2$,

would require $n \gtrsim 5$ to reproduce the observed hardness ratio, but result in too low *XMM-Newton* EPIC/pn count rates. We also explored models with mass loss rates and circumstellar density profiles in the ranges $0.1 \leq \dot{M}_{-5} \leq 30$ and $1.1 \leq s \leq 2.9$, respectively. Models with $\dot{M}_{-5} \lesssim 0.5$, while predicting consistent hardness ratios, are unreasonable as their cooling times are much greater than the age of SN 2001gd. Models with $s \gtrsim 2.4$ predict significantly lower *XMM-Newton* EPIC/pn count rates than observed. Models with $\dot{M}_{-5} \gtrsim 15$ (middle panel in Fig. 6) or $s \lesssim 1.4$ (bottom panel in Fig. 6) have hardness ratios between the energy band above 2 keV and the total *XMM-Newton* energy band that are $\gtrsim 0.6$, well above the observed hardness ratio of $0.1^{+0.2}_{-0.1}$ (see Sect. 2.3). Therefore, models with $\dot{M}_{-5} \lesssim 0.5$ or $\dot{M}_{-5} \gtrsim 15$, and models with $s \lesssim 1.4$ or $s \gtrsim 2.4$ seem less likely to describe the X-ray emission from SN 2001gd than the model shown in the top panel of Fig. 6.

At the adopted distance of 13.1 Mpc, the unabsorbed flux from SN 2001gd is $F_X = (7 \pm 2) \times 10^{-14}$ ergs cm $^{-2}$ s $^{-1}$ in the 0.3–5 keV band, which corresponds to a luminosity of $L_X = 4\pi D^2 F_X = (1.4 \pm 0.4) \times 10^{39} D_{13}^2$ ergs s $^{-1}$, where $D = 13.1 D_{13}$ Mpc is the distance to the supernova. The above results are in agreement with expectations from X-ray emission from Type II supernovae (e.g., Fransson et al. 1996), and seem to favour a relatively shallow ejecta density profile and a mass-loss rate about a factor of two lower than for SN 1993J.

The 2 July 2001 *XMM-Newton* observations of SN 2001gd did not yield detectable X-ray emission, but can be used to derive an upper limit of the isotropic X-ray luminosity of SN 2001gd at that time. The 3σ upper limit on this luminosity is $L_X = 7.4 \times 10^{38}$ erg s $^{-1}$. Note, however, that this upper limit to the X-ray luminosity was obtained with a significantly shorter exposure time, and with a much higher background X-ray emission level, compared to that for the observations on 18 December 2002.

Finally, the expected monochromatic flux density at 4.9 GHz on 18 December 2002 ($t - t_0 = 472$ d) was $\approx (2.5 \pm 0.3)$ mJy. Using $\alpha = -1.0$ from our best-fit VLA spectrum on 8 April 2003, we obtain an isotropic radio luminosity of $L_R = (8 \pm 2) \times 10^{36} D_{13}^2$ ergs s $^{-1}$ between 1.4 and 43 GHz. The values of L_X and L_R put SN 2001gd close to SN 1993J (Chevalier 2003) regarding radio and X-ray luminosities, in agreement with the fact that SN 2001gd displayed a very similar behaviour to SN 1993J in the optical band.

4.3 Expansion of SN 2001gd

The VLBI images of SN 2001gd at 8.4 GHz (Fig. 4) show a compact, unresolved radio emitting structure. Therefore, we resorted to model fitting to estimate the supernova angular diameter, θ , at each epoch. For this purpose, we used the model fitting procedure included in the Caltech DIFMAP package, which fits a given model directly to the real and imaginary parts of the observed interferometric visibilities, using the Levenberg-Marquardt non-linear least squares minimization technique. Inspired by the findings for SN 1993J (e.g., Marcaide et al. 1995a,b, 1997; Bartel et al. 2000), we assumed spherical symmetry in our model fits, and considered the following models: (i) an optically thin

Table 2. Angular diameter estimates of SN 2001gd

Model	Angular diameter (μ as)	
	2002.48	2003.27
OPTICALLY THIN SPHERE	390 ± 80	440 ± 100
UNIFORMLY BRIGHT DISK	350 ± 60	410 ± 80
OPTICALLY THIN SHELL [†]	330 ± 60	370 ± 80

[†] The shell width is 25% the outer radius.

sphere; (ii) a uniformly bright, circular disk; and (iii) an optically thin shell of width 25 % its outer shell radius (e.g. Marscher 1985). Table 2 summarizes our results, where the uncertainties (1σ) represent one statistical standard deviation plus an estimate of modelling errors. All three models give similarly good fits to the (u, v) data ($\chi^2_{\text{red}} = 0.8 - 0.9$), so in principle we cannot rule out any of them. Our angular diameter estimates nominally suggest a relatively strong deceleration in the expansion of SN 2001gd, but values of the deceleration parameter m ($\theta \propto t^m$) between 0 and 1 are all within the uncertainties, and therefore we cannot draw any conclusion from our data.

4.4 Energy budget and magnetic field in SN 2001gd

The high brightness temperatures inferred from our VLBI observations for SN 2001gd [$(5.3 \pm 1.2) \times 10^8$ K on 26 June 2002, and $(1.1 \pm 0.3) \times 10^8$ K on 8 April 2003], indicate a non-thermal, synchrotron origin for the radio emission from SN 2001gd. We can estimate a minimum total energy in relativistic particles and fields, and an equipartition magnetic field for SN 2001gd, by assuming equipartition between fields and particles. The minimum total energy and its equipartition magnetic field are (Pacholczyk 1970):

$$E_{\min} = c_{13} (1 + \psi)^{4/7} \phi^{3/7} R^{9/7} L_R^{4/7} \quad (2)$$

$$B_{\min} = (4.5 c_{12}/\phi)^{2/7} (1 + \psi)^{2/7} R^{-6/7} L_R^{2/7} \quad (3)$$

where L_R is the radio luminosity of the source; R , its linear radius; c_{12} and c_{13} , slowly-varying functions of the spectral index, α (Pacholczyk 1970); ϕ , the filling factor of fields and particles; and ψ the ratio of the (total) heavy particle energy to the electron energy. This ratio depends on the mechanism that generates the relativistic electrons and ranges from $\psi \approx 1$ to $\psi = m_p/m_e \approx 2000$, where m_p and m_e are the proton and electron mass, respectively.

From our VLA observations on 8 April 2003, we determined a spectral index $\alpha = -1.0 \pm 0.1$ ($S_\nu \propto \nu^\alpha$; see Sect. 4.1) between 1.4 and 43 GHz, and $S_{8.4\text{GHz}} = 1.02 \pm 0.05$ mJy. With these values, we obtain $L_R = (6.0 \pm 0.3) \times 10^{36} D_{13}^2$ ergs s $^{-1}$ between 1.4 and 43 GHz. We used $\phi = 0.6 \phi_{0.6}$ in our calculations, which corresponds approximately to the filling factor for the shell model in Table 2. In any case, the estimates of E_{\min} and B_{\min} are relatively insensitive to the precise value of ϕ . The radius of SN 2001gd on 8 April 2003 is, for the shell model, $R = 3.6 \times 10^{16} D_{13} \theta_{185}$ cm, where θ_{185} is the angular radius of the supernova in units of 185 mas. With these values, we get from Eq. (2) and (3)

$$E_{\min} \approx 1.8 \times 10^{46} (1 + \psi)^{4/7} \phi_{0.6}^{3/7} \theta_{185}^{9/7} D_{13}^{17/7} \text{ ergs}$$

$$B_{\min} \approx 40 (1 + \psi)^{2/7} \phi_{0.6}^{-2/7} \theta_{185}^{-6/7} D_{13}^{-2/7} \text{ mG}$$

Since $1 \lesssim \psi \lesssim 2000$, E_{\min} is in the range $(2.6 \times 10^{46} - 1.4 \times 10^{48})$ erg, and the equipartition magnetic field in the range $(50-350)$ mG. Thus, for an energy of 10^{51} ergs for the explosion of SN 2001gd, the fraction of energy necessary to power the radio emission of SN 2001gd is quite modest. The upper range of the equipartition magnetic field is lower than, but not far from, the lowest part of the range of values obtained for SN 1993J at similar radii ($B \approx 1.7$ G, Fransson & Björnsson 1998; $B \approx 0.5$ G, Pérez-Torres et al. 2001).

Since the kinetic energy density in the wind is likely larger than the circumstellar magnetic field energy density (e.g., Fransson & Björnsson 1998), we have $\rho_{\text{csm}} v_{\text{w}}^2/2 \gtrsim B_{\text{csm}}^2/8\pi$, where ρ_{csm} and B_{csm} are typical of the density and magnetic field in the circumstellar medium, respectively. By assuming a standard wind density profile ($\rho \propto r^{-2}$), we can write the above expression as

$$B_{\text{csm}} \lesssim (\dot{M} v_w)^{1/2} r^{-1} \approx 2.5 (\dot{M}_{-5} v_{10})^{1/2} r_{16}^{-1} \text{ mG} \quad (4)$$

where $r_{16} = r/10^{16}$ cm. For $r_{16} = 3.6$ and $\dot{M}_{-5} = 2.5$, we obtain $B_{\text{csm}} \lesssim 1$ mG, which is a factor about 50 to 350 times smaller than the equipartition field, and shows that the magnetic field inferred for SN 2001gd cannot originate solely by compression of the existing circumstellar magnetic field, which would increase the field only by a factor of four (e.g., Dyson & Williams 1980). Large amplification factors of the magnetic field have also been found for other radio SNe, e.g., SN1993J (amplification factors of a few hundred; Fransson & Björnsson 1998, Pérez-Torres et al. 2001), or SN 1986J (amplification factors in the range 40–300; Pérez-Torres et al. 2002). Thus, if equipartition between fields and particles exists, amplification mechanisms other than compression of the circumstellar magnetic field need to be invoked, e.g., turbulent amplification (Chevalier 1982; Chevalier & Blondin 1995), to explain the radio emission from supernovae.

5 SUMMARY

We have presented the results of the first two 8.4 GHz very-long-baseline interferometry observations of SN 2001gd in NGC 5033, complemented with VLA and *XMM-Newton* observations. We summarize our main results as follows:

- The radio structure of SN 2001gd is not resolved, either on 2002.48 ($t - t_0 = 295$ days; $t_0 = 3$ September 2001) or on 2003.27 ($t - t_0 = 582$ days). We used the interferometric visibility data to estimate the angular sizes for the supernova, as well as constraints on its expansion speed from optical measurements. While our data nominally suggest the possibility of a relatively strong deceleration in the expansion of SN 2001gd ($m \ll 1$, $\theta \propto t^m$), solutions with $m = 1$ are also permitted, and therefore we cannot draw any conclusion from these data.

- Our VLA data on 8 April 2003 can be well fit by an optically thin, synchrotron spectrum ($\alpha = -1.0 \pm 0.1$; $S_{\nu} \propto \nu^{\alpha}$), which is partially absorbed by thermal electrons. The radio spectrum and the light curve at 1.4 GHz indicate that the synchrotron turnover frequency is near 1 GHz. We obtain a supernova flux density of (1.02 ± 0.05) mJy at the observing

frequency of 8.4 GHz. At an adopted distance of 13.1 Mpc to NGC 5033, this flux density implies an isotropic radio luminosity of $(6.0 \pm 0.3) \times 10^{36}$ ergs s $^{-1}$ between 1.4 and 43 GHz. We also used our best-fit to the VLA radio spectrum to infer the most likely ranges for the electron temperature in the wind, T_e , and the mass-loss rate, \dot{M} . From our VLA observations on 8 April 2003, we find $T_e = (3 - 20) \times 10^4$ K, and $\dot{M} = (2 - 10) \times 10^{-5} \text{ M}_{\odot} \text{ yr}^{-1}$. (Note the constraint on the combination of these values; see Sect. 4.1 and 4.2.)

- By assuming equipartition between fields and particles, we estimate a minimum total energy in relativistic particles and magnetic fields in the supernova shell of $E_{\min} \approx (0.3 - 14) \times 10^{47}$ erg, which corresponds to an equipartition average magnetic field there of $B_{\min} \approx (50 - 350)$ mG. We find that the average magnetic field in the circumstellar wind of SN 2001gd is $B_{\text{csm}} \lesssim 1$ mG at a radius from the center of the supernova explosion of $\approx 3.6 \times 10^{16}$ cm. Since compression of this existing magnetic field by the supernova shock front could enhance it by only a factor of four, powerful amplification mechanisms must then be acting in SN 2001gd, to account for the magnetic fields responsible for the synchrotron radio emission.

- We used *XMM-Newton* archival data to estimate the X-ray flux of SN 2001gd on 2 July 2001 and 18 December 2002. The data from the X-ray observations on 2 July 2001 are below the noise level, while we detected SN 2001gd on 18 December 2002, with a flux of $(7 \pm 2) \times 10^{-14}$ erg cm $^{-2}$ s $^{-1}$ in the 0.3–5 keV band. The emission is chiefly from a soft component (<2 keV), associated with the reverse shock of the supernova. The corresponding isotropic X-ray luminosity is $L_{\text{x}} = (1.4 \pm 0.4) \times 10^{39}$ erg s $^{-1}$ in the 0.3–5 keV band. The X-ray spectrum is consistent with expectations from X-ray emission from Type II supernovae (e.g., Fransson et al. 1996), and suggests the interaction of a relatively shallow supernova ejecta density profile ($\rho_{\text{ej}} \sim r^{-n}$; $n \approx 10$), with a standard circumstellar wind density profile ($\rho_{\text{csm}} \sim r^{-s}$; $s \approx 2.0$), characterized by a presupernova mass-loss rate of $\dot{M} \approx 2.5 \times 10^{-5} \text{ M}_{\odot} \text{ yr}^{-1}$ for SN 2001gd.

SN 2001gd resembles SN 1993J in its radio and X-ray emission, indicating that a similar circumstellar interaction is taking place. Since available radio supernovae for VLBI studies are so rare, it is important that the few of them that allow such studies be monitored if we are to better understand the radio supernova phenomenon. Further VLBI observing epochs of SN 2001gd are necessary to trace the expansion history of the supernova, and to determine whether SN 2001gd is decelerating. However, the task is most challenging, as SN 2001gd appears to fade very quickly in radio. We estimate that SN 2001gd will have a flux density at 8.4 GHz of about 0.3–0.4 mJy around March–April 2005. Therefore, the chances of a successful radio imaging of SN 2001gd are small, and will necessarily require the use of an array including the world's most sensitive antennas.

ACKNOWLEDGMENTS

This research was partially funded by the grants AYA2001-2147-C02-01 and AYA2002-00897 of the Spanish Ministerio de Ciencia y Tecnología. MAPT and MAG are supported by the Spanish National programme Ramón y Cajal. KWW wishes to thank the Office of Naval Research for the

6.1 funding supporting this research. We thank NRAO, the Max-Planck-Institut für Radioastronomie, and the Istituto di Radioastronomia for supporting our observing campaigns. We thank an anonymous referee for useful comments and suggestions, which significantly improved our manuscript. NRAO is a facility of the USA National Science Foundation operated under cooperative agreement by Associated Universities, Inc. We made use of the NASA Astrophysics Data System Abstract Service. The Digitized Sky Surveys were produced at the Space Telescope Science Institute under U.S. Government grant NAG W-2166. The images of these surveys are based on photographic data obtained using the Oschin Schmidt Telescope on Palomar Mountain and the UK Schmidt Telescope. The plates were processed into the present compressed digital form with the permission of these institutions.

REFERENCES

Bartel N., et al., 2000, *Science*, 287, 112

Baron E., Hauschildt P. H., Branch D. 1994, *ApJ*, 426, 334

Beasley A. J., Conway J., 1995, in Zensus J. A., Diamond P. J., Napier, P. J., eds, *ASP Conf. Ser.*, Vol. 82, VLBI Phase-Referencing. *Astron. Soc. Pac.*, San Francisco, p. 328

Chevalier R. A., 1982, *ApJ*, 259, 302

Chevalier R. A., Fransson C., 1994, *ApJ*, 420, 268

Chevalier R. A., Blondin J. M., 1995, *ApJ*, 442, 312

Chevalier R. A., 2003, in Hillebrandt W., Leibundgut B., eds, *From Twilight to Highlight: The Physics of Supernovae*. Springer, Berlin, p. 299

Dyson J. E., Williams D. A., 1980, *Physics of the interstellar medium* (New York: John Wiley & Sons)

Falco, E. E., et al., Updated Zwicky Catalog (UZC), 1999, *PASP*, 111, 438

Fransson C., Lundqvist P., Chevalier R., 1996, *ApJ*, 461, 993

Fransson C., Björnsson C.-I., 1998, *ApJ*, 509, 861

Hewitt A., Burbidge G., 1989, A new optical catalog of Quasi-Stellar Objects.

Lundqvist P., Fransson C., 1988, *A&A*, 192, 221

Marcaide J. M., et al., 1995a, *Nature*, 373, 44

Marcaide J. M., et al., 1995b, *Science*, 270, 1475

Marcaide J. M., et al., 1997, *ApJ*, 486, L31

Marcaide J. M., et al., 2002, in Ros E., Porcas R. W., Lobanov A. P., Zensus J. A., ed., *Proceedings of the 6th European VLBI Network Symposium*. Max-Planck Institut für Radioastronomie, p. 239

Marscher A. P., 1985, in Bartel N., ed., *Supernovae as Distance Indicators*, Lecture Notes in Physics, 224. Springer, Berlin, p. 130

Matheson T., et al., 2000, *AJ*, 120, 1487

Matheson T., et al., 2001, *IAU Circ.* 7765

Mucciarelli P., Zampieri L., Pastorello A., 2004, to appear in Turatto M., Shea W., Benetti S., Zampieri L., ed., *Proc. of the International Conference “1604-2004: Supernovae as Cosmological Lighthouses”*. *ASP conference Series* ([astro-ph/0411755](#))

Nakano S., et al., 2001, *IAU Circ.*, 7761

Pacholczyk A. G., 1970, *Radio Astrophysics* (San Francisco: Freeman)

Pérez-Torres M. A., Alberdi A., Marcaide, J. M., 2001, *A&A*, 374, 997

Pérez-Torres M. A., et al., 2002, *MNRAS*, 335, L23

Pérez-Torres M. A., et al., 2005, in Marcaide J. M., Weiler K. W., eds, *Proc. IAU Col. 192, Cosmic Explosions: On the 10th Anniversary of SN 1993J*. Springer, Berlin, p. 97

Shepherd M. C., Pearson T. J., Taylor G. B., 1995, *BAAS*, 26, 987

Strüder L., et al., 2001, *A&A*, 365, L18

Stockdale C. J., et al., 2002, *IAU Circ.*, 7830

Stockdale C. J., et al., 2003, *ApJ*, 592, 900

Turner M. J. L., et al., 2001, *A&A*, 365, L27